

## Development of a fluorescent probe for the detection of hPD-L1

Xinyu Li,<sup>1,‡</sup> Xiaoming Huang,<sup>1,‡</sup> Liqian Zhang,<sup>1</sup> Yang Cong,<sup>1</sup> Guangwei Zhao,<sup>1</sup> Jingru Liang,<sup>1</sup> Hao Chen,<sup>1</sup> Haimei Li,<sup>1</sup> Limei Chen,<sup>1</sup> and Jinhua Dong<sup>1,2,\*</sup>

Key Laboratory for Biological Medicine in Shandong Universities, Weifang Key Laboratory for Antibody Medicine, School of Life Science and Technology, Weifang Medical University, Weifang 261053, China<sup>1</sup> and World Research Hub Initiative, Institute of Innovative Research, Tokyo Institute of Technology, Yokohama 226-8503, Japan<sup>2</sup>

Received 22 April 2020; accepted 16 June 2020  
Available online xxx

**Interaction of human programmed death factor-1 (hPD-1) of T cells and one of its ligands hPD-L1 which is expressed on cancer cells suppresses effector T cell functions. Studies showed that the hPD-1/hPD-L1 pathway is associated with killing mechanisms of tumor cells evading the immune system. Immunotherapy based on the checkpoint inhibitor on hPD-1 has been an important approach to treat cancer; however, not all cancer cells over-express hPD-L1. Detection of hPD-L1 over-expression in cancer cells may be a key factor for deciding on whether immunotherapy should be conducted. In the present study, we produced recombinant hPD-1 using *Escherichia coli*, and created a fluorescent probe termed quenched hPD-1 (QPD-1) for the detection of hPD-L1. We found that hPD-1 can quench fluorescence of carboxytetramethylrhodamine labeled on its N-terminal and QPD-1 is a convenient tool to rapidly detect hPD-L1 with a limit of detection of 10 nM and detectable range of 10 nM–1000 nM. QPD-1 may also function as a probe to screen for hPD-L1 over-expressing tumor cells and promote appropriate medical procedure through tumor immunotherapy.**

© 2020, The Society for Biotechnology, Japan. All rights reserved.

[**Key words:** Immunotherapy; Cancer; Human PD-1; Human PD-L1; Fluorescent probe; Quench]

Human programmed death factor-1 (hPD-1) of T cells, first reported by Ishida et al. (1), is an important factor involved in negative immune responses. Its ligands are hPD-L1 and hPD-L2 (2); hPD-L1 has a broad range and is typically highly expressed in tumor cells (Fig. 1A; PDB ID: 4zqk). Previous studies showed that microenvironments produced by proliferation and aggregation of tumor cells can induce over-expression of hPD-L1 on the surface of tumor cell membranes; this typically results in suppression of effector T cell functioning due to an interaction with hPD-1, which enables tumor cells to evade the immune system (3). In cancer treatments, blocking the hPD-1/hPD-L1 pathway functionally restores the functions of attenuated T cells (4).

Currently, antibodies that block the hPD-1/hPD-L1 signaling system are available. However, although hPD-1/hPD-L1 monoclonal antibodies have shown promising results in clinical anti-tumor applications, treatment strategies including hPD-1/hPD-L1 antibodies and immune checkpoint inhibitor monotherapy are not suitable for every cancer patient. An overall objective response rate of 20%–40% was reported (5), and 9%–29% of the patients showed signs of disease progression after receiving hPD-1 monoclonal antibody therapy (3,6). Studies showed that various tumor cells are affected by a variety of regulatory factors in different tumor

microenvironments. Protein expression kinetics, cut-off values, and tumor type are important factors determining hPD-L1 expression on the cell surface (7,8). Therefore, measuring hPD-L1 expression levels in cancer cells may be a decisive factor in immunotherapy. Detection of hPD-L1 was limited as enzyme-linked immunosorbent assay (ELISA), Western blot and immunohistochemistry (IHC). Chou et al. (9) have developed a flow-proteomic platform for analyzing protein concentration for measure the protein concentration including hPD-L1 in cells or tissue. Liu et al. (10) have developed another technology based on surface plasmon resonance but without requirement of nanostructure fabrication to detect hPD-L1 in serum. However, at present, hPD-L1 expression levels are clinically assessed during treatment of non-small cell lung cancer with hPD-L1 inhibitors using IHC, which emphasizes the need for additional means of detection.

Biosensors have been commonly used for medical diagnosis and scientific research. At present, most types of biosensors require a complex experimental setup, and they are typically time-consuming and somewhat imprecise (11). Recently, a new and powerful homogeneous immunoprobe termed Quenchbody was developed, and its functioning is based on a novel principle: Quenchbody is an antibody fragment labeled with a fluorescent dye, and it can be used to measure abundance of specific compounds based on fluorescence intensity changes which indicate antigen-antibody binding (12,13). As antibodies are highly specific for their respective antigens, most studies using probes focused on antigen-antibody reaction, whereas few probes based on protein-protein interaction studied so far. Here, we studied interactions of hPD-1 and a fluorescent dye label on its N-terminal. We developed an hPD-L1-dependent immunosensor named Quenched PD-1

\* Corresponding author at: Key Laboratory for Biological Medicine in Shandong Universities, Weifang Key Laboratory for Antibody Medicine, School of Life Science and Technology, Weifang Medical University, Weifang 261053, China. Tel.: +86 5365462455.

E-mail addresses: [dongjh@wfm.edu.cn](mailto:dongjh@wfm.edu.cn), [dongjinhua@pe.res.titech.ac.jp](mailto:dongjinhua@pe.res.titech.ac.jp) (J. Dong).

‡ The first two authors contributed equally to this work.

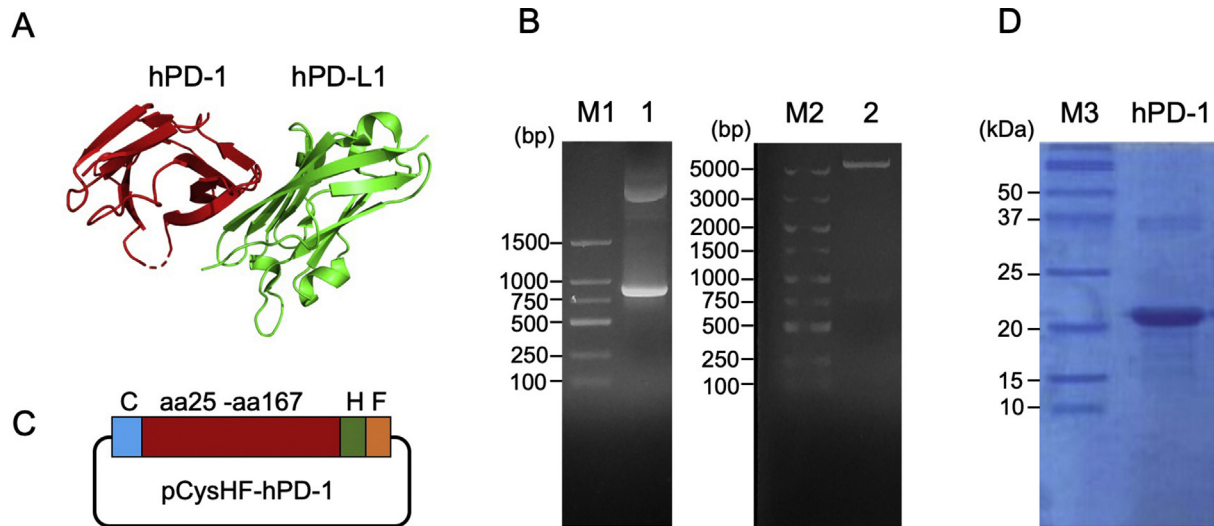


FIG. 1. Construction of a human PD-1 expression vector and protein expression. (A) Structure of hPD-1 and hPD-L1 (PDB ID: 4zqk); (B) agarose electrophoresis of the amplified gene coding for hPD-1 and the enzyme-digested vector; (C) pCysHF-hPD-1 structure; (D) SDS-PAGE analysis of purified hPD-1. C, Cys-tag; H, his-tag; F, Flag-tag; M1, DNA marker 100–1500 bp; lane 1, purified hPD-1 gene; M2, DNA marker 100–5000 bp; lane 2, digested pCysHF plasmid; M3, Precision Plus Protein Unstained Standards.

(QPD-1). Fluorescent intensity of QPD-1 increases upon binding to hPD-L1, therefore it can be used for the detection of hPD-L1 and screening cancer cells that over-express hPD-L1 in order to decide whether patients are suitable for hPD-1 immunotherapy. This technique has a wide range of potential applications such as detection of hPD-L1 for diagnosis of tumor diseases, screening for hPD-L1 over-expressing tumor cells, and investigating the functions of hPD-L1 in tumor metastasis, among others.

## MATERIALS AND METHODS

**Materials** An optimized DNA sequence encoding human hPD-1 (NCBI accession number NP\_005009.2; PDCD1) was designed and synthesized by Shanghai Sango Biotechnology Co. Ltd. (Shanghai, China). XL10-Gold *Escherichia coli* cells are used for general cloning and SHuffle T7 express lysY competent *E. coli* cells are used for protein expression (New England Biolabs, Ipswich, MA, USA) (14,15). Restriction endonuclease *AgeI* and *NotI* were purchased from New England Biolabs, and ligation reagent Ligation High Ver. 2 and polymerase enzymes KOD-Plus-Neo and Blend Taq were purchased from Toyobo Biochemicals (Osaka, Japan). Primers were synthesized by Shanghai Sango Biotechnology Co. Ltd. Agarose, ampicillin, and Isopropyl  $\beta$ -D-thiogalactoside (IPTG) were obtained from Beijing Solarbio Technology Co., Ltd (Beijing, China). Precision Plus Protein Dual Color Standards and Precision Plus Protein Unstained Standards were purchased from Bio-Rad (Hercules, CA, USA).

**Amplification of the hPD-1 gene** Human PD-1 protein consists of a signal peptide, an extracellular domain, and a transmembrane domain. Plasmid pUC57-hPD-1 containing a gene coding extracellular domain of hPD-1 was synthesized by Shanghai Sango Biotechnology Co. Ltd. The hPD-1 gene was amplified by polymerase chain reaction (PCR) using primers M13+ (AGGGTTTCCCAGTCACG) and M13- (GAGCGGATAACAATTTCACAC). PCR reactions were performed using KOD-Plus-Neo polymerase and under the following reaction conditions: DNA was denatured at 94°C for 2 min followed by 30 cycles of denaturation at 98°C for 30 s, primer annealing at 55°C for 30 s, and extension at 68°C for 1 min. PCR products were visualized by agarose gel electrophoresis. Target DNA fragments were purified using a SanPrep DNA gel recovery kit (Shanghai Sango Biotechnology, Co. Ltd.), and concentration of recovered DNA was measured using a microphotometer.

**Construction of an hPD-1 expression vector** Fifty nanograms of in-house produced pCysHF were used to transform competent XL10-Gold *E. coli* cells which were then plated on Luria broth (LB) medium containing ampicillin and were cultured at 37°C for 12 h. Single colonies were picked and placed in 4 mL LB liquid medium containing 100  $\mu$ g/mL ampicillin and were cultured at 37°C overnight. After that, plasmids were extracted using a SanPrep plasmid DNA extraction kit (Shanghai Sango Biotechnology, Co. Ltd.). Plasmid pCysHF and hPD-1 genes were digested using *AgeI* and *NotI*, followed by separation using

agarose gel electrophoresis, and purification. Digested pCysHF and hPD-1 genes were then ligated using Ligation High Ver. 2 and introduced into XL10-Gold *E. coli* cells which were incubated at 37°C overnight. Single colonies were picked and presence of the hPD-1 gene was confirmed by PCR using the T7 promoter (TAATACGACTCACTATAGGG) and T7 terminator (GCTAGTTATTGCTCAGCGG) primers. The sequence of inserted gene was confirmed by sequence analysis. Plasmid containing the appropriate sequence was designated pCysHF-hPD-1.

**Expression and purification of hPD-1 protein** Fifty nanograms pCysHF-hPD-1 were used to transform SHuffle T7 express lysY *E. coli* cells which were then cultured on LB solid medium plates containing 100  $\mu$ g/mL ampicillin at 37°C overnight. Single colonies were transplanted to LB liquid medium containing ampicillin and were cultured in shock at 30°C until OD<sub>600</sub> was 0.4. IPTG at a final concentration of 1 mM was added to the culture, and incubation was continued in a shaker at 200 rpm and 16°C. *E. coli* cells cultured overnight were centrifuged at 8000  $\times$  g for 20 min at 4°C, and the pellet was collected. Cells were then re-suspended in 10 mL binding/washing buffer (20 mM sodium phosphate, 500 mM sodium chloride, 5 mM imidazole; pH 8.0) for ultrasonic disruption for 30 min (3 s ultrasonication intervals with 2 s break). After ultrasonication, samples were centrifuged at 8000  $\times$  g for 20 min at 4°C, and the supernatant was collected.

One hundred microliter of Ni-NTA Sefinose Resin (Shanghai Sango Biotechnology, Co. Ltd.) was equilibrated using binding/washing buffer and packed to an empty column with diameter of 20 mm, followed by application of the protein solution and washing. Elution buffer (20 mM sodium phosphate, 500 mM sodium chloride, 500 mM imidazole; pH 8.0) was added to column, and purified samples were collected. Ten microliters per sample were used for dodecyl sulfate sodium salt-polyacrylamide gel electrophoresis (SDS-PAGE) analysis (16). Highly pure samples with high protein concentration were dialyzed against a phosphate-buffered saline (PBS) buffer.

**Enzyme-linked immunosorbent assay** To confirm activity of recombinant hPD-1, an ELISA with a phage-displaying antibody was carried out as shown in Fig. 2A. One hundred microliters of hPD-1 or bovine serum albumin (BSA; 2.0  $\mu$ g/mL) as a negative control were added to wells of a 96-well microplate, and reactions were incubated at 4°C overnight. After this, protein solutions were removed, and well surfaces were blocked using 2% skimmed milk in PBS (MPBS) after washing with a solution of PBS containing 0.5% Tween20 (PBST) three times. The phage-displaying anti-hPD-1 antibody nivolumab was added to the wells, and reactions were incubated at room temperature for 1 h. After this, the phage-antibody solution was removed, and horseradish peroxidase (HRP) conjugated anti-M13 antibody (GE Healthcare, Tokyo, Japan) was added to the wells, followed by incubation for 1 h and washing with PBST thrice. For color development, 100  $\mu$ L TMBZ (3,3',5,5'-tetramethylbenzidine; Sigma, St Louis, MO, USA) solution in CH<sub>3</sub>COONa containing H<sub>2</sub>O<sub>2</sub> was added to each well after washing. Following incubation for 10 min, 10% H<sub>2</sub>SO<sub>4</sub> was added to terminate the reaction. Absorbance was measured at 450 nm and at 630 nm as a control. To confirm binding of hPD-1 to hPD-L1, hPD-L1 at a concentration of 2.0  $\mu$ g/mL was added to some samples with the anti-hPD-1 phage antibody.

To confirm hPD-L1-binding activity of QPD-1, 100  $\mu$ L QPD-1 at 2.0  $\mu$ g/mL was used to coat wells of a 96-well microplate. BSA at 2.0  $\mu$ g/mL was used as a control.

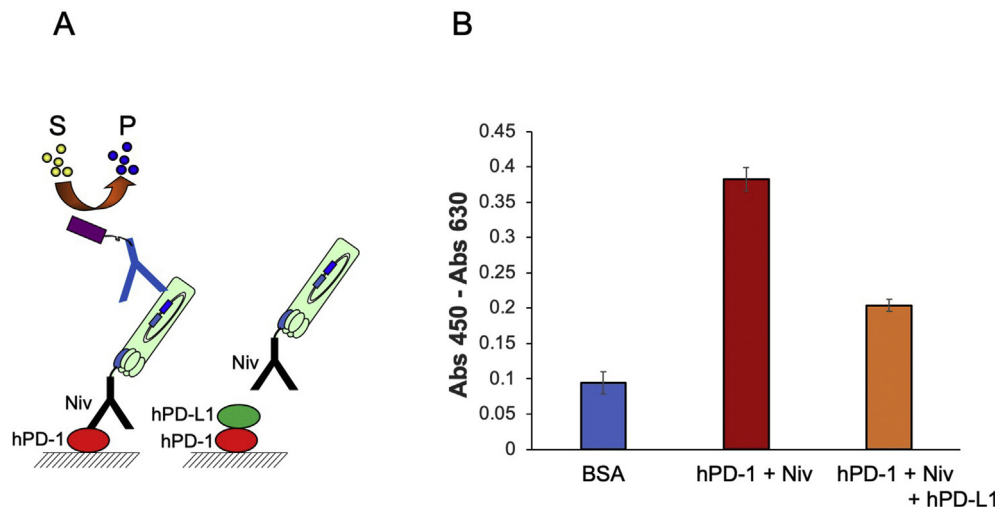


FIG. 2. Binding activity of recombinant hPD-1 to anti-hPD-1 antibody and hPD-L1. (A) Phage-based ELISA; (B) ELISA results of binding of hPD-1 with anti-hPD-1 antibody and with hPD-L1. S, substrate; P, enzymatic reaction products; BSA, bovine serum albumin; Niv, nivolumab.

After blocking, 100  $\mu$ L hPD-L1 solution at 2.0  $\mu$ g/mL was added to each well. After incubation and washing, mouse anti-hPD-L1 IgG and HRP/rabbit anti-mouse IgG antibody were added successively. Color development and absorbance measurements were performed as described above.

**Preparation of quenched hPD-1 (QPD-1)** Purified hPD-1 was dialyzed with PBST and was treated with tris(2-carboxyethyl) phosphine hydrochloride (TCEP) at a final concentration of 0.5 mM by shaking for 20 min. A solution of 4-azidobenzoic acid at a final concentration of 2 mM was added to the reaction mixture which was then incubated on ice for 10 min. After this, carboxytetramethylrhodamine (TAMRA)-C5-maleimide (Fig. 3A) was added at a 10-fold molar ratio of the protein, and the reaction was incubated in the dark for 2 h. The labeling mixture was then purified using anti-FLAG M2 beads (Thermo Fisher Scientific, Waltham, MA, USA) which is for purification of protein containing a FLAG tag (DYKDDDDK) according to the manufacturer's instructions. In brief, anti-FLAG beads (20  $\mu$ L) were washed using PBS and were then added to the samples for subsequent incubation in the dark for 2 h. Beads were then washed three times using PBST. Bead-bound QPD-1 protein was eluted using 100  $\mu$ L 3  $\times$  FLAG peptide at 150  $\mu$ g/mL. Ten microliters of purified sample were used for SDS-PAGE, followed by observation of fluorescence of the QPD-1 in a fluorescence imager (GELmieu) (Wako, Osaka, Japan) and visible light imaging after staining with Coomassie Brilliant Blue. The labeling efficiency of QPD-1 was calculated by titrating the fluorescence concentration of QPD-1 solution with a TAMRA standard curve and dividing it by protein concentration. Samples were stored in the dark at  $-20^{\circ}$ C until further use.

**Quenching and de-quenching of the QPD-1 probe** QPD-1 at 10 nM was added to PBST or denaturant solution containing 7 M guanidine hydrochloride and 2 M DL-dithiothreitol (GdnHCl/DTT), which can completely disintegrate protein structure and release fluorescent dye molecules (Fig. 4A). Fluorescence intensity of QPD-1 in PBST and in denaturant solution was measured using a F4600 fluorescence spectrophotometer (HITACHI, Japan), and whether quenching occurred can be determined by comparing fluorescence intensities. hPD-L1 was added to QPD-1 solution in PBST at final concentrations of 0, 1, 10, 50, 100, 300, 900, 1000 and 3000 nM, and fluorescence spectra were measured (Fig. 5A). Quenching efficiency, de-quenching, and QPD-1 fluorescence intensity effects on hPD-L1 addition were examined in denaturant solution, in PBST, and in PBST with serial concentrations of hPD-L1. A dose-response curve was fitted to a four-parameter logistic equation by using GraphPad Prism 8 (GraphPad Software, San Diego, CA, USA). The limit of detection (LOD) is calculated as the concentration corresponding to the average blank value plus three times the standard deviation.

## RESULTS

**Construction of vector and protein expression** The hPD-1 gene was amplified from a synthetic plasmid by PCR, separated by agarose gel electrophoresis and visualized under a fluorescent

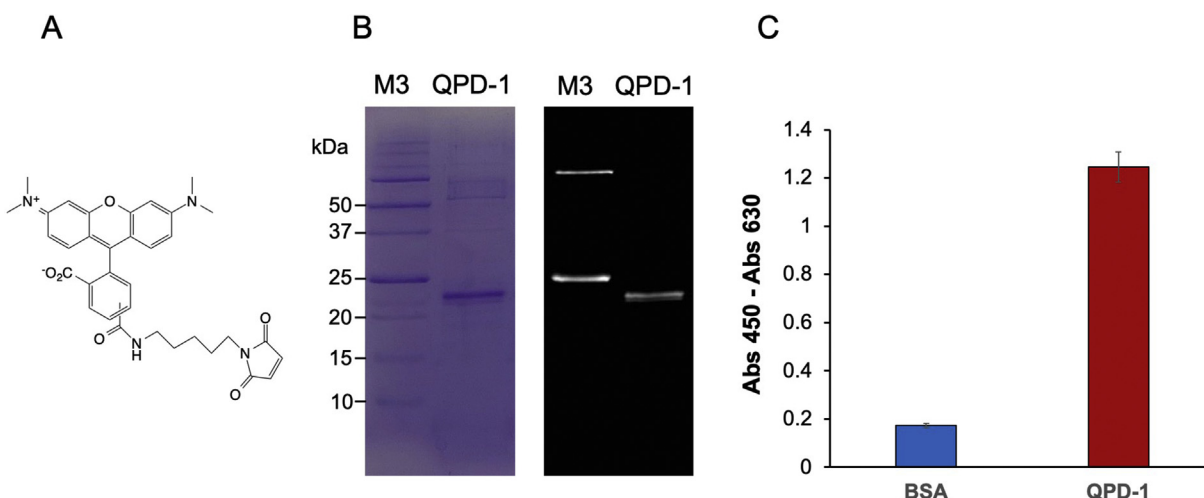


FIG. 3. Preparation, SDS-PAGE, and ELISA analysis of QPD-1. (A) Structure of TAMRA-maleimide-C5; (B) SDS-PAGE analysis of QPD-1; (C) ELISA analysis of hPD-L1-binding activity of QPD-1. M3, Precise Plus Protein Dual Color Standards. (For interpretation of the references to color in this figure legend, the reader is referred to the Web version of this article.)

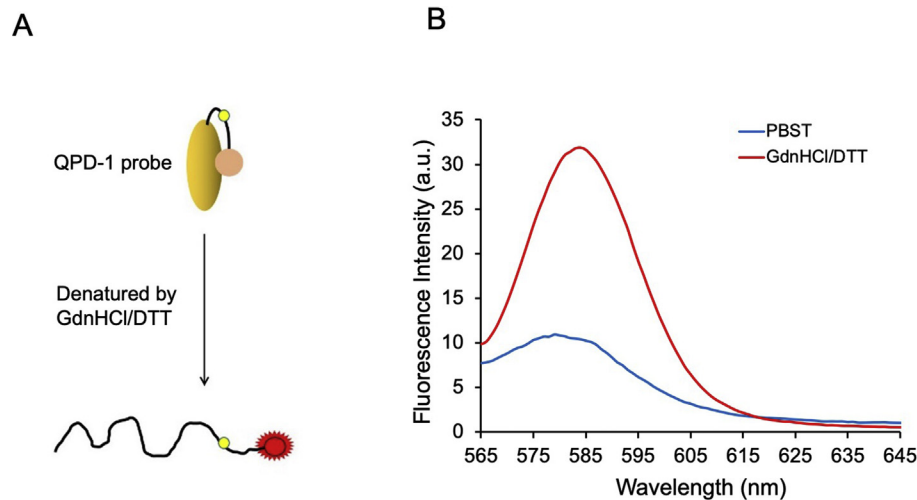


FIG. 4. Quenching analysis of the QPD-1 probe. (A) Schematic diagram for QPD-1 denaturation; (B) fluorescent spectra of QPD-1 in PBST and in denaturant solution.

photography. As shown in Fig. 1B, a distinct DNA fragment of 800 bp was observed, which was the predicted length of the target product, indicating that the hPD-1 gene was amplified successfully. The protein expression plasmid pCysHF was digested, and two bands were observed after gel electrophoresis as shown in Fig. 1B. The longer DNA fragment was collected and used to ligated with the digested hPD-1 gene to produce the expression vector pCysHF-hPD-1. As shown in Fig. 1C, the vector expresses a fusion protein of hPD-1 with an additional peptide (MAQIEVNCSNET) at its N-terminal that enhances the protein expression (17). The peptide contains a cysteine amino acid that can react with fluorescent dyes which carry a maleimide group. At the C-terminal of the fusion protein, a HIS tag and a FLAG tag were attached for protein purification.

*E. coli* cells containing a recombinant plasmid were cultured and induced by adding IPTG, and proteins were purified using Ni-NTA Sefinose Resin. Purified hPD-1 was analyzed using SDS-PAGE. As shown in Fig. 1D, a protein band of 21 kDa was presumed to be recombinant hPD-1 protein which, according to calculations, has a molecular weight of 19.8 kDa. This difference in molecular weight

may be because of consistent mobility of amino acids. hPD-L1 binding activity of hPD-1 was confirmed using an ELISA with a phage-displaying nivolumab antibody. As shown in Fig. 2B, hPD-1-coated wells showed strong absorbance, whereas BSA-coated wells produced weak signals, suggesting that recombinant hPD-1 is active against the anti-hPD-1 antibody. In contrast, samples containing additional hPD-L1 protein produced weaker signals than the samples without hPD-L1, suggesting that hPD-1 binds hPD-L1.

**Preparation of QPD-1** The N-terminal of purified hPD-1 was labeled using TAMRA-maleimide-C5 (Fig. 3A) and was then purified again using an anti-FLAG resin to remove any unbound TAMRA-maleimide-C5. Purified QPD-1 was analyzed using SDS-PAGE. As shown in Fig. 3B, Coomassie Brilliant Blue staining showed a distinct band with a size of 23 kDa, which corresponded to the expected size of QPD-1. Fluorescence imaging confirmed successful fluorescence labelling of the protein. An ELISA with immobilized QPD-1 was performed to confirm hPD-L1 binding activity of QPD-1. After adding hPD-L1, anti-hPD-L1 antibodies and HRP conjugated anti-mouse antibody, the assay was

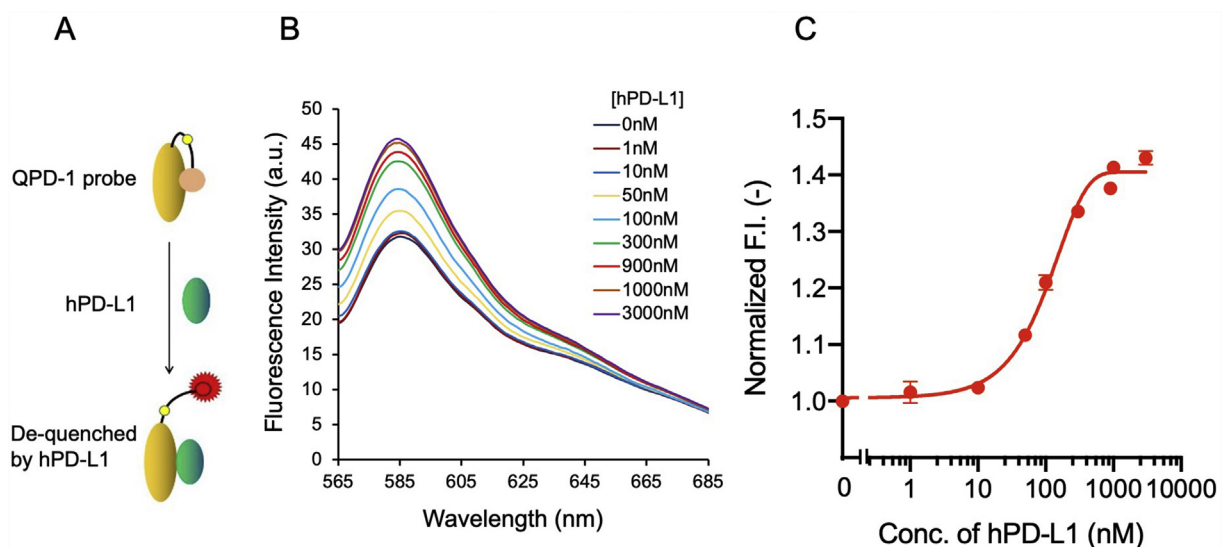


FIG. 5. Detection of hPD-L1 with QPD-1. (A) Schematic diagram for detection of hPD-L1 using QPD-1; (B) fluorescent spectra of QPD-1 in a dilution series of hPD-L1; (C) dose-response curve for detection of hPD-L1 using QPD-1.

developed. As shown in Fig. 3C, the absorbance at 450 nm differed significantly between wells coated with QPD-1 and those coated with BSA, suggesting that QPD-1 actively binds hPD-L1. The labeling efficiency of QPD-1 calculated by dividing the fluorescence concentration by the protein concentration was 86%, indicating that 86 out of 100 QPD-1 molecules have successfully labeled with TAMRA.

**hPD-1 quenched TAMRA dye** QPD-1 was structurally disintegrated using the denaturing reagent, and changes in fluorescence were recorded. Fluorescence spectra of QPD-1 in GdnHCl/DTT and PBST are shown in Fig. 4B. Fluorescence intensity of QPD-1 was more than 3.06-fold stronger in denaturing solution than in PBST, suggesting that TAMRA fluorescence was quenched by the hPD-1 protein. When TAMRA is linked with hPD-1, it may move within the hPD-1 protein and its fluorescence may be quenched by certain amino acids of hPD-1 such as tryptophan; however, after structural disintegration of the protein, the quenching effect was removed leading to increased fluorescence of QPD-1.

**Detection of hPD-L1 using QPD-1** As fluorescence of labeled TAMRA was quenched by hPD-1 in QPD-1, we investigated whether QPD-1 can be used to detect hPD-L1. We added hPD-1 to QPD-1 solution in a dilution series and measured changes in fluorescence (Fig. 5A). Fluorescence spectra of QPD-1 upon addition of hPD-L1 are shown in Fig. 5B. With increasing concentrations of hPD-L1, fluorescence intensity of QPD-1 at 580 nm increased (Fig. 5C). A standard dose-response curve with EC<sub>50</sub> of 110 nM, detectable range of 10 nM–1000 nM, and limit detection of 10 nM hPD-1 was obtained. Fluorescence intensity increased to 1.43-fold maximum compared to that without hPD-L1 addition. These results suggest that QPD-1 can be used as a fluorescence probe for hPD-L1 detection.

## DISCUSSION

Quenchbody, which is an antibody fragment labeled with fluorescent dyes, has been a universal technique for monitoring drug residues in environmental and food samples (13). In this application, dye fluorescence is typically quenched by conserved tryptophan in antibody molecules, and when Quenchbody binds to its antigen, the fluorescent dye molecules moved to the outside of the antibody and the quenching effect is removed, resulting in increased fluorescence intensity. This technology has been used to detect not only environmental pollutants such as deoxynivalenol (18) and imidacloprid which is a neonicotinoid insecticide (19), but also peptides (20) and diverse proteins such as hemagglutinin of an influenza virus (21) and claudin1 and HER2 which are cancer biomarkers (22,23).

Besides antigen-antibody interaction, there are many molecular interactions such as ligand-receptor or protein-protein interactions. Convenient and fast detection of these interactions may be important for research on various physiological functions and for developing therapeutic agents. hPD-L1 is highly expressed in many cancer cells (24) but is typically under-expressed in antigen-presenting cells, non-hematopoietic cells such as vascular endothelial cells, islet cells, and sites of increased immunity functions such as placenta, testes, and eyes (25). Therefore, hPD-L1 can be used as a tumor biomarker, and detection of hPD-1 may help with early diagnoses of cancer. High expression of hPD-L1 in a tumor microenvironment suggests that patients are more likely to benefit from blocking hPD-1/hPD-L1 binding. Therefore, high expression levels of hPD-L1 indicate stronger effects of hPD-1/hPD-L1 inhibitors. Taken together, it is crucial to monitor hPD-L1 expression levels on the cell surface.

So far, detection methods of hPD-L1 were limited to IHC that takes several hours (26). Here, we developed a quenched hPD-1

probe for convenient, fast, and accurate detection of hPD-L1. A fluorescent dye, TAMRA, was used to label recombinant hPD-1 at a specific position, and fluorescence of TAMRA was quenched by tryptophan residues through photo-induced electron transfer (27,28). However, when QPD-1 binds to its ligand hPD-L1, the fluorescent dye is moved by hPD-L1 to the protein surface which removes the quenching effect and elicits fluorescence. There are no washing steps needed for the assay and the assay can be finished only by mixing of sample and probe solutions and measuring the fluorescence intensity within few minutes. This QPD-1 assay is a convenient and fast method for detecting hPD-L1. The EC<sub>50</sub> of the assay was 110 nM, higher than the equilibrium dissociation constant  $K_D$  value of hPD-1/hPD-L1 binding reported previously (29). The reason might be the design and producing process of hPD-1 protein, suggesting the function of the probe may be further improved by protein engineering.

According to literature, tryptophan residues provide electrons to fluorescent dye molecules around them to cause quenching (12). Two tryptophan residues are close to the binding site of hPD-1 with hPD-L1 and may function as fluorescence quenchers. To increase the fluorescence signal upon binding hPD-L1, we plan to mutate some amino acids to tryptophan residues in future, which may cause greater photo-induced electron transfer with fluorescent dyes, thereby increasing probe sensitivity. Interactions between tryptophan residues and fluorescent dyes are also affected by the distance between dye and quencher. We thus plan to enhance the quenching effect by increasing the length of the linker between the label site and the N-terminal of the protein. As an alternative to the fluorescent dye TAMRA, rhodamine dyes such as R110, ATTO520, ATTO655, and oxamide dyes should also be tested for this purpose in future studies.

QPD-1 can be used in medical tests to determine whether tumor patients should be subjected to tumor immunotherapy with hPD-1/hPD-L1 system antibodies. Furthermore, this method can also be used for fluorescent staining of tumor cells in scientific research to improve distinguishability of tumor cells and to rapidly and accurately identify tumor cells.

## ACKNOWLEDGMENTS

This study was partly funded by the National Natural Science Foundation of China (Grant Number: 21775064), Shandong Provincial Natural Science Foundation (Grant Number: ZR2017MB037), and Science and Technology Planning Project of Weifang City, Shandong Province of China (Grant Number: 2020YQFK014).

## References

1. Ishida, Y., Agata, Y., Shibahara, K., and Honjo, T.: Induced expression of PD-1, a novel member of the immunoglobulin gene superfamily, upon programmed cell death, *EMBO J.*, **11**, 3887–3895 (1992).
2. Dong, H., Zhu, G., Tamada, K., and Chen, L.: B7-H1, a third member of the B7 family, co-stimulates T-cell proliferation and interleukin-10 secretion, *Nat. Med.*, **5**, 1365–1369 (1999).
3. Saada-Bouazid, E., Defaucheux, C., Karabadjian, A., Coloma, V. P., Servois, V., Paoletti, X., Even, C., Fayette, J., Guigay, J., Lohr, D., and other 4 authors: Hyperprogression during anti-PD-1/PD-L1 therapy in patients with recurrent and/or metastatic head and neck squamous cell carcinoma, *Ann. Oncol.*, **28**, 1605–1611 (2017).
4. Freeman, G. J., Long, A. J., Iwai, Y., Bourque, K., Chernova, T., Nishimura, H., Fitz, L. J., Malenkovich, N., Okazaki, T., Byrne, M. C., and other 9 authors: Engagement of the PD-1 immunoinhibitory receptor by a novel B7 family member leads to negative regulation of lymphocyte activation, *J. Exp. Med.*, **192**, 1027–1034 (2000).
5. Iwai, Y., Hamanishi, J., Chamoto, K., and Honjo, T.: Cancer immunotherapies targeting the PD-1 signaling pathway, *J. Biomed. Sci.*, **24**, 26 (2017).
6. Champiat, S., Derclé, L., Ammari, S., Massard, C., Hollebecque, A., Postel-Vinay, S., Chaput, N., Eggermont, A., Marabelle, A., Soria, J. C., and Ferte, C.: Hyperprogressive disease is a new pattern of progression in cancer patients treated by anti-PD-1/PD-L1, *Clin. Cancer Res.*, **23**, 1920–1928 (2017).

7. **Cottrell, T. R. and Taube, J. M.:** PD-L1 and emerging biomarkers in immune checkpoint blockade therapy, *Canc. J.*, **24**, 41–46 (2018).
8. **Gibney, G. T., Weiner, L. M., and Atkins, M. B.:** Predictive biomarkers for checkpoint inhibitor-based immunotherapy, *Lancet Oncol.*, **17**, e542–e551 (2016).
9. **Chou, C. K., Huang, P. J., Tsou, P. H., Wei, Y., Lee, H. H., Wang, Y. N., Liu, Y. L., Shi, C., Yeh, H. C., Kameoka, J., and Hung, M. C.:** A flow-proteometric platform for analyzing protein concentration (FAP): proof of concept for quantification of PD-L1 protein in cells and tissues, *Biosens. Bioelectron.*, **117**, 97–103 (2018).
10. **Liu, C., Zeng, X., An, Z., Yang, Y., Eisenbaum, M., Gu, X., Jornet, J. M., Dy, G. K., Reid, M. E., Gan, Q., and Wu, Y.:** Sensitive detection of exosomal proteins via a compact surface plasmon resonance biosensor for cancer diagnosis, *ACS Sens.*, **3**, 1471–1479 (2018).
11. **Ueda, H. and Dong, J.:** From fluorescence polarization to Quenchbody: recent progress in fluorescent reagentless biosensors based on antibody and other binding proteins, *Biochim. Biophys. Acta*, **1844**, 1951–1959 (2014).
12. **Abe, R., Ohashi, H., Iijima, I., Ihara, M., Takagi, H., Hohsaka, T., and Ueda, H.:** "Quenchbodies": quench-based antibody probes that show antigen-dependent fluorescence, *J. Am. Chem. Soc.*, **133**, 17386–17394 (2011).
13. **Abe, R., Jeong, H. J., Arakawa, D., Dong, J., Ohashi, H., Kaigome, R., Saiki, F., Yamane, K., Takagi, H., and Ueda, H.:** Ultra Q-bodies: quench-based antibody probes that utilize dye-dye interactions with enhanced antigen-dependent fluorescence, *Sci. Rep.*, **4**, 4640 (2014).
14. **Bessette, P. H., Aslund, F., Beckwith, J., and Georgiou, G.:** Efficient folding of proteins with multiple disulfide bonds in the *Escherichia coli* cytoplasm, *Proc. Natl. Acad. Sci. USA*, **96**, 13703–13708 (1999).
15. **Levy, R., Weiss, R., Chen, G., Iverson, B. L., and Georgiou, G.:** Production of correctly folded Fab antibody fragment in the cytoplasm of *Escherichia coli* *trx*B *gor* mutants via the coexpression of molecular chaperones, *Protein Expr. Purif.*, **23**, 338–347 (2001).
16. **Laemmli, U. K.:** Cleavage of structural proteins during the assembly of the head of bacteriophage T4, *Nature*, **227**, 680–685 (1970).
17. **Abe, R., Shiraga, K., Ebisu, S., Takagi, H., and Hohsaka, T.:** Incorporation of fluorescent non-natural amino acids into N-terminal tag of proteins in cell-free translation and its dependence on position and neighboring codons, *J. Biosci. Bioeng.*, **110**, 32–38 (2010).
18. **Yoshinari, T., Ohashi, H., Abe, R., Kaigome, R., Ohkawa, H., and Sugita-Konishi, Y.:** Development of a rapid method for the quantitative determination of deoxynivalenol using Quenchbody, *Anal. Chim. Acta*, **888**, 126–130 (2015).
19. **Zhao, S., Dong, J., Jeong, H. J., Okumura, K., and Ueda, H.:** Rapid detection of the neonicotinoid insecticide imidacloprid using a quenchbody assay, *Anal. Bioanal. Chem.*, **410**, 4219–4226 (2018).
20. **Dong, J., Fujita, R., Zako, T., and Ueda, H.:** Construction of Quenchbodies to detect and image amyloid beta oligomers, *Anal. Biochem.*, **550**, 61–67 (2018).
21. **Jeong, H. J., Dong, J., and Ueda, H.:** Single-step detection of the influenza virus hemagglutinin using bacterially-produced quenchbodies, *Sensors*, **19**, 52 (2018).
22. **Dong, J., Oka, Y., Jeong, H. J., Ohmuro-Matsuyama, Y., and Ueda, H.:** Detection and destruction of HER2-positive cancer cells by Ultra Quenchbody-siRNA complex, *Biotechnol. Bioeng.*, **117**, 1259–1269 (2020).
23. **Jeong, H. J., Kawamura, T., Iida, M., Kawahigashi, Y., Takigawa, M., Ohmuro-Matsuyama, Y., Chung, C. I., Dong, J., Kondoh, M., and Ueda, H.:** Development of a quenchbody for the detection and imaging of the cancer-related tight-junction-associated membrane protein claudin, *Anal. Chem.*, **89**, 10783–10789 (2017).
24. **Patel, S. P. and Kurzrock, R.:** PD-L1 expression as a predictive biomarker in cancer immunotherapy, *Mol. Canc. Therapeut.*, **14**, 847–856 (2015).
25. **Shukuya, T. and Carbone, D. P.:** Predictive markers for the efficacy of anti-PD-1/PD-L1 antibodies in lung cancer, *J. Thorac. Oncol.*, **11**, 976–988 (2016).
26. **Ancevski Hunter, K., Socinski, M. A., and Villaruz, L. C.:** PD-L1 testing in guiding patient selection for PD-1/PD-L1 inhibitor therapy in lung cancer, *Mol. Diagn. Ther.*, **22**, 1–10 (2018).
27. **Vaiana, A. C., Neuweiler, H., Schulz, A., Wolfrum, J., Sauer, M., and Smith, J. C.:** Fluorescence quenching of dyes by tryptophan: interactions at atomic detail from combination of experiment and computer simulation, *J. Am. Chem. Soc.*, **125**, 14564–14572 (2003).
28. **Marme, N., Knemeyer, J. P., Sauer, M., and Wolfrum, J.:** Inter- and intramolecular fluorescence quenching of organic dyes by tryptophan, *Bioconjugate Chem.*, **14**, 1133–1139 (2003).
29. **Ghiotto, M., Gauthier, L., Serriari, N., Pastor, S., Truneh, A., Nunes, J. A., and Olive, D.:** PD-L1 and PD-L2 differ in their molecular mechanisms of interaction with PD-1, *Int. Immunol.*, **22**, 651–660 (2010).